Finite Element Modeling and Analysis of CMOS-SAW Sensors

Onur Tigli*, Mona E. Zaghloul**

*School of Engineering and Computer Science, Washington State University, Vancouver, WA, USA, tigli@wsu.edu

** Electrical and Computer Engineering Dept., George Washington University, Washington, DC, USA, zaghloul@gwu.edu

ABSTRACT

Finite element modeling and performance analysis of Surface Acoustic Wave (SAW) devices that are developed in CMOS (Complementary Metal Oxide Semiconductor) technology are presented. CMOS-SAW devices were designed, fabricated and characterized as a biosensor for breast cancer biomarker detection. A detailed 3D model with 18 CMOS layers and a structured finite element (FE) analyses methodology are laid out to extract the acoustic behavior of the substrate and the piezoelectric material of interest, zinc oxide (ZnO). A three-step analysis encompassing modal, harmonic and transient simulations is detailed. Experimental characterization results for the fabricated CMOS-SAW devices with operating frequency of 322.7 MHz show close agreement to the FE simulations with only 0.8 % deviations for operation frequency. Displacement and stress/strain maps for wave propagation are also presented. The results demonstrate that commercial FEM toolsets can provide valuable insight into understanding acousto-electric interactions and wave characteristics or can readily be used for accurate design parameter extraction through reliable pre-fabrication simulation of SAW device performance.

Keywords: SAW, CMOS, MEMS, FEM

1 INTRODUCTION

There is a significant interest in developing structured methods to understand electrical, acoustic, and mechanical behaviors of SAW devices in general. This interest is coupled with the desire to produce rapid and reliable design parameter extraction with accurate post-fabrication performance analyses that can be used to emulate actual device operation. These interests have been addressed for conventional SAW devices by the development of dedicated special programs in recent years [1]. Most of these efforts were limited in the types of devices they can model and performance metrics they can simulate.

A novel approach to SAW device fabrication is introduced in our previous work [2], [3]. As demonstrated by the results of this work, CMOS-SAW devices constitute a viable alternative to traditional SAW devices with their improved performance and ease of mass fabrication promise. This paper aims to layout a methodological use of commercially available FEM software toolset to model and analyze performance of such novel devices in particular and SAW devices in general.

During the design phase of SAW devices, it is necessary to get information on fundamental parameters such as operating frequency, insertion loss, and electromechanical conversion factor. Considering the recent advancements in commercially available structured FEM toolsets, all of this essential information and detailed insight on wave generation or propagation can easily be obtained. Equivalent circuit models traditionally provide a good starting point for designing SAW devices. The results obtained from such efforts in our previous work [2], [3] allow the determination of primary design parameters such as the center frequency, 3dB bandwidth, insertion loss, and transfer characteristics at and around the frequency of operation. However, it makes several approximations and assumptions to convert the acoustic properties to electrical representations. Although this approach provides a fast and relatively accurate analysis of the performance characteristics, it is always desirable to gain insight into electromechanical interactions and fundamental physics of acoustic wave generation or propagation. Therefore, in order to fully understand the acoustoelectric interactions that take place in the piezoelectric material and to closely investigate the behavior of the interdigitated transducers (IDT) when designed in CMOS, we carried out a comprehensive finite element analysis (FEA) for the devices and architectures that were developed in [2]-[4].

2 PROCESS AND 3D MODELING

As a first step, an 18 step CMOS fabrication sequence was defined. The sequence is designed to closely resemble the sequence of interest: AMI Semiconductor's 0.5 µm. This n-well CMOS process has 3 metal layers, 2 poly layers, and an NPN option. There are 6 different layers of oxide in this process. Every deposition and etching step requires distinct masks to be designed. The masks designed for the CMOS fabrication are imported into the layout editor to reflect all the dimensions in correct form. The mask layouts are presented elsewhere [3]. Fig. 1 (a) depicts a typical 3D model of the CMOS-SAW delay line obtained

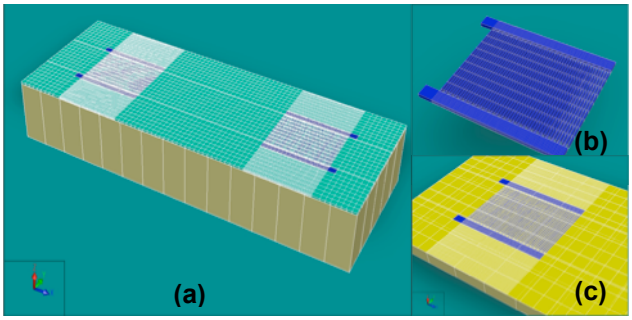

Fig. 1. (a) Meshed CMOS-SAW delay line with input/output IDTs and transparent display of top piezoelectric layer (b) Close-up snapshot of the meshed IDT with 5 µm manhattan brick elements (c) Close-up showing the IDT and the delay line meshing differences with the top piezoelectric layer hidden for clarity.

by using the CMOS process steps. Fig. 1 (c), on the other hand, shows a close up of a simplified version of the model in Fig. 1 (a). This simplification essentially eliminates any non-functional architectural complexities to obtain better simulation performance and more effective modeling.

Once the 3-D models are constructed, the structures were meshed for finite element based analysis. The correct choice of meshing element type and size is an optimization problem. This problem carries a trade-off between accurate results and reasonable simulation costs. Therefore, an incremental meshing optimization was carried out to obtain the most suitable element types and sizes. A very coarse meshing (e.g. element size of 50 µm) is applied to the substrate region and a fine meshing (e.g. element size of 5 µm) is carried out for the rest of the layers. Due to the well-defined sidewalls and edges of the IDT structures, *manhattan* and *extruded bricks* with parabolic elements yielded the best performance for the meshing. The final optimized mesh resulted in 329,222 *vertices*, 132,125 *edges*, 114,596 *faces* and 32,485 *regions*.

3 ANALYSES AND SIMULATION

The finite element analyses of SAW devices focus primarily on steady state responses and modal deformations of the layers [5]. Although this focus provides sufficient information on the frequency response of the devices, it overlooks important performance parameters such as phase velocity, transient displacements, stress/strain distributions and voltage induction. Here, we carried out detailed performance investigation in three categories for all of the designed architectures: *modal*, *harmonic* and *transient*. Modal and harmonic results were used to analyze frequency responses and displacements, whereas transient analyses were used to investigate the actual wave generation/propagation, stress/strain distributions and voltage induction.

Modal analysis is used to compute the natural resonant frequency of the mechanical structure at equilibrium. This is achieved by calculating the unbounded response of an undamped mechanical structure to a bounded excitation [7]. These natural resonant frequencies determine when the system will have its maximum response to an intended or unintended (noise) input. Since the modal analysis is performed on an undamped system, the amplitudes of the mode shapes does not reflect the actual amplitudes of the motion and are normalized to a maximum deflection of 1 µm. For the modal analysis of the CMOS-SAW device, the frequency of interest is set to be 320 MHz with 5 modes. The solution includes mode shapes, displacement distributions, and generalized mass values. Maximum displacement for the SAW occurs at a resonant frequency of 319.998 MHz, which closely agrees with previously calculated and simulated center frequencies [3].

The second most insightful analysis in FEM of CMOS-SAW devices is the steady-state responses to harmonic excitation. We used an electromechanical solver to perform a dynamic analysis with a sinusoidal load. The responses of the devices still include steady-state components in frequency domain. The harmonic analysis followed by a modal analysis uses the equation of motion for the *αth* mode [6]

$$\ddot{q}_\alpha + c_\alpha \dot{q}_\alpha + \omega_\alpha{}^2 q_\alpha = \frac{1}{m_\alpha} f_\alpha e^{j\Omega t} \qquad (1)$$

where

q_α: the amplitude of mode α
c_α: the damping coefficient associated with this mode
ω_α: the undamped frequency of this mode
m_α: the generalized mass associated with the αth mode
f_α : the amplitude of forcing associated with the mode
Ω : forcing frequency

The eigenmodes calculated in the modal analysis is

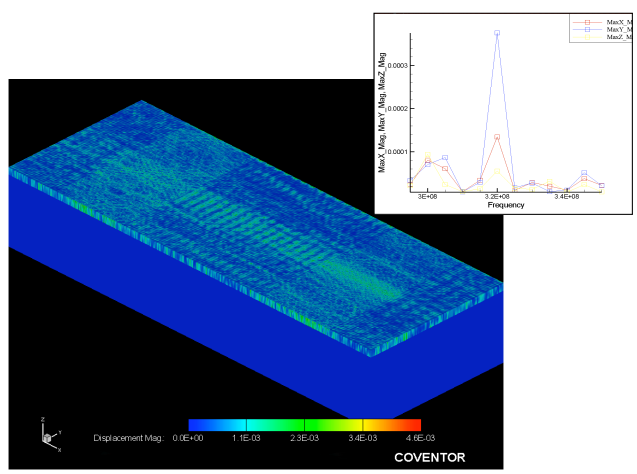

Fig. 2. Displacement map for the CMOS-SAW delay line at the center frequency f_c = 320 MHz. Harmonic response in frequency domain (inset)

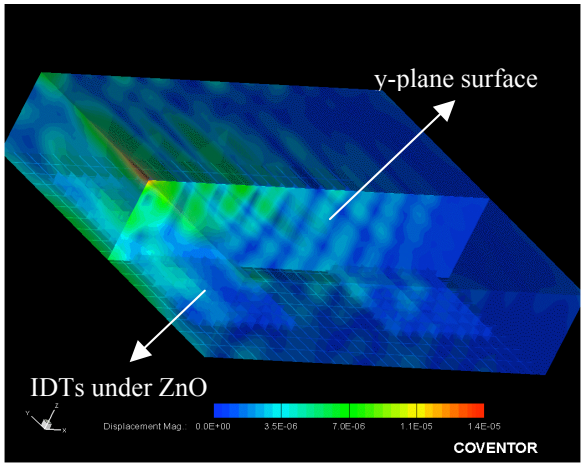

(a)

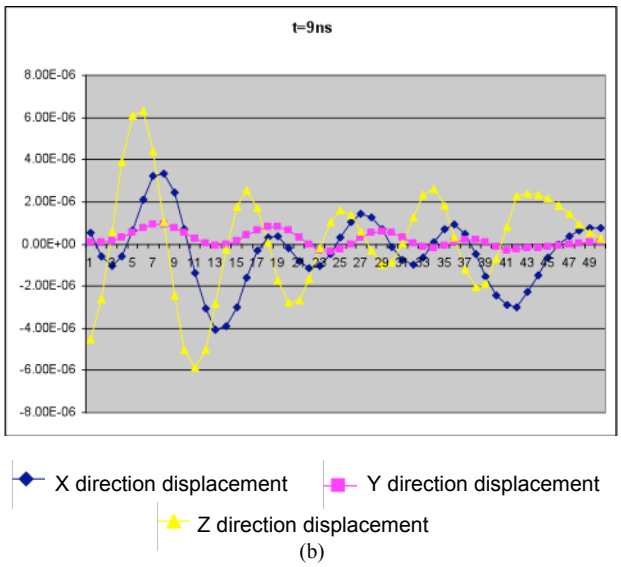

(b)

Fig. 3. (a) Displacement vector distribution at 9 ns for the CMOS-SAW delay line (b) Displacement vectors in (x,y,z) for the acoustic wave propagation on the iso surface plane

plugged into (1) to solve the steady state harmonic responses for user specified frequencies. As determined by the modal analysis results, the frequency of interest is centered at 319.998 MHz. Therefore a frequency range of 55 MHz is set spanning 295 MHz – 355 MHz interval. For this simulation 12 different modes were determined. The maximum displacements in every direction occur at the center frequency of 320 MHz. Fig. 2 shows the displacement map and the corresponding frequency response for the harmonic analysis.

Modal and harmonic analysis help reveal important CMOS-SAW device design parameters such as center frequency, mode distance, generalized mass, and frequency response for the undamped eigenfrequencies. However, to gain more insight into the characteristics of the piezoelectric material of interest, further analysis is required. A new mesh, which is a downsized version of the previous one, was developed for *transient* analysis purposes. Since the primary point of interest is to analyze the SAW generation/propagation within the piezoelectric material of ZnO, a much smaller IDT model can be employed to give effectively the same wave characteristics. A transient analysis of 10 ns was carried out with solver timesteps of 0.25 ns and output timesteps of 0.5 ns. A periodic sine wave input of amplitude 1 V was applied as the input excitation. Stress/strain, displacement, and wave/voltage propagation simulation data were collected. Fig. 3 shows the distribution of the displacement vectors in the ZnO layer for a 10 ns simulation. Only the discrete time snapshot at 9 ns is presented here. Based on the readings from the figure, the acoustic wave generated at the input IDT travels a distance of 20 µm in 5.2 ns. This translates into a phase velocity of 20 µm /5.2 ns = 3846.15 m/s which closely agrees with the previously used velocity figure of 3850 m/s [2]. An iso-surface was generated within the ZnO layer to extract data for the propagation of the wave. As it was also evidenced by the harmonic analysis, the wave penetrates the whole depth of 3 µm for a full swing while preserving its periodicity without any distortion. The displacement results for the iso-surface are plotted in Fig. 3 (b) for the same discrete time used for Fig. 3 (a). This demonstrates that the waves in all directions preserve their periodicity as they propagate through the delay line to reach the output IDT at 10 ns.

4 DEVICE FABRICATION AND CHARACTERIZATION

The novel CMOS-SAW devices were fabricated in AMI 0.5 µm 3 metal/2 poly technology through MOSIS [7]. Each die contains two SAW delay lines that are aligned perpendicular to each other. The period and the derivative parameters such as finger spacing or width are dictated by the design rules of the technology in use. The modeling and design parameter extraction of the devices were detailed in [3]. The layout of the devices employs ideas that are completely compatible with any other commercial CMOS process. Therefore, seamless migration to any other feature size as well as any other CMOS process can be easily achieved. Three step novel post-processing methods were designed, optimized, and characterized in our previous work [3], [8]. Fig. 4 (a) shows a scanning electron microscopy (SEM) snapshot of a typical finished CMOS-SAW device die. The overall device performance strongly depends on precise definition of the IDT fingers and their alignment with respect to each other. This was achieved by control of etching parameters as detailed in [8]. The device performances are analyzed using HP 8712ET, 300 kHz – 1300 MHz, RF Network Analyzer. The experiment results show a center frequency at 322.7 MHz with an insertion loss of 39.48 dB and a 3dB bandwidth of 38.12 MHz. Fig. 4 (b) shows a typical CMOS-SAW S_{21} transmission response that was obtained by electrical characterization.

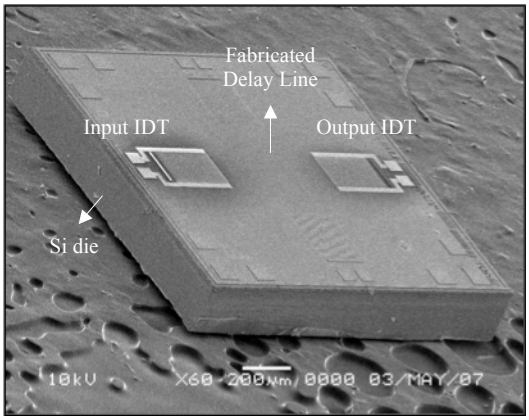

(a)

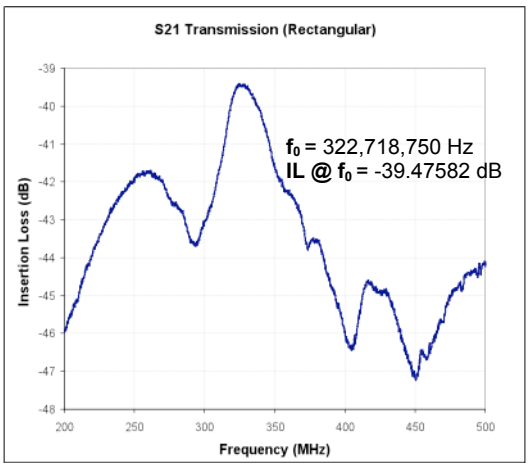

(b)

Fig. 4. (a) SEM snapshot for a typical finished CMOS-SAW die (b) Typical S_{21} Transmission transfer characteristics for a CMOS-SAW device.

5 CONCLUSION

A detailed finite element modeling and performance analysis of SAW devices in CMOS technology was carried out. We used a commercial MEMS software toolset [6] to gain insight into stress-strain relations, displacement distributions, and electromechanical conversion factors. We also studied performance metrics such as insertion loss, acoustic wave behavior and transient wave characteristics.

In order to evaluate the accuracy and precision of the FEM work that was completed in this paper, we also carried out a comparative investigation. The FEM simulation results were compared with electrical characterization data for the actual fabricated CMOS-SAW devices [8] and crossed field equivalence models that were developed based on Mason equivalent circuitry [9]. Table I summarizes the results from each data set. Experimental characterization results for the fabricated CMOS-SAW devices with operating frequency of 322.7 MHz show close agreement to the FE simulations with 0.8 % and 17 % deviations for operation frequency and 3dB bandwidth respectively. FEM results also show -6 % deviations for maximum rejection bandwidth when compared to the SAW Mason equivalent circuit based crossed-field model. These results demonstrate that the FEM methodology followed in this paper presents much more accurate and reliable source of information on SAW device characteristics in general when compared to equivalent circuit based modeling. In addition, it provides larger sets of data to extract real-time behavior of acoustic wave devices through high-resolution visual representations. This aspect can prove to be highly desirable in case of complex architectures that employ multi-layer structures and variety of materials.

TABLE I
COMPARATIVE DEVICE CHARACTERISTICS OF CMOS-SAW

	Equivalent Circuit	FEM Sim.	Experimental
Center Frequency f_0 (MHz)	318.4	320.0	322.7
Insertion Loss at f_0 (MHz)	-9.11	-32.76	-39.48
3 dB bandwidth (MHz)	23.84	n/a	38.12
Max. rejection bandwidth (MHz)	42.56	40.00	56.24
Shape Factor	2.12	n/a	1.92

REFERENCES

[1] M. Koshiba, N. Shichishima, Kazuhiro Ohbuchi, and Yasuhide Tsuji "Software for a multilayered surface acoustic wave device based on the finite element method and coupling-of-modes theory" *J. J. Appl. Phys.*, pp. 3060-3063, 1997.

[2] O. Tigli, M. Zaghloul, "Design and Fabrication of a Novel SAW Biochemical Sensor in CMOS," *IEEE Sensors, Special Session: CMOS Based Sensors*, Irvine, CA, Oct. 2005.

[3] O. Tigli, M. Zaghloul, "A Novel SAW Device in CMOS: Design, Modeling and Fabrication," *IEEE Sensors Journal*, pp. 214-223, Feb. 2007.

[4] O. Tigli, M. Zaghloul, "A Novel Circular SAW (Surface Acoustic Wave) Device in CMOS", *Proc. of IEEE Sensors*, Atlanta, GA, pp. 474-477, Oct. 2007.

[5] Thomas, R., Johannes, T. W., Ruile, W., and Weigel, R., "Determination of Phase Velocity and Attenuation of Surface Acoustic Waves with Improved Accuracy," *IEEE Ultrasonics Syposium*, pp. 277-282, Oct. 1998.

[6] Coventor, Inc., CoventorWare "Using CoventorWare Analyzer," Tutorial, 2006.

[7] [Online] MOSIS, "Low-cost prototyping and small-volume production service for VLSI circuit development," www.mosis.com , 2008.

[8] O. Tigli, M. Zaghloul, "Design, Modeling and Characterization of a Novel Circular Surface Acoustic Wave Device," *IEEE Sensors Journal*, Vol. 8, No. 11, pp. 1807-1815, Nov. 2008.

[9] Mason, W. P., "Electromechanical Transducers and Wave Filters," *van Nostrand-Reinhold 2nd Edition*, Princeton, New Jersey, pp. 399-409, 1948.